RESEARCH ARTICLE

Molecular
Carcinogenesis WILEY

Transcriptome profiling reveals that VNPP433-3β, the lead next-generation galeterone analog inhibits prostate cancer stem cells by downregulating epithelial–mesenchymal transition and stem cell markers

Elizabeth Thomas[1,2] | Retheesh S. Thankan[1,3,4] | Puranik Purushottamachar[1,2] | Weiliang Huang[5] | Maureen A. Kane[5] | Yuji Zhang[6,7] | Nicholas Ambulos[8] | David J. Weber[2,9,10] | Vincent C. O. Njar[1,2,10]

[1]Department of Pharmacology, University of Maryland School of Medicine, Baltimore, Maryland, USA

[2]The Center for Biomolecular Therapeutics, University of Maryland School of Medicine, Baltimore, Maryland, USA

[3]Isoprene Pharmaceuticals Inc., Baltimore, Maryland, USA

[4]Flavocure Biotech, Baltimore, Maryland, USA

[5]Department of Pharmaceutical Sciences, University of Maryland School of Pharmacy, Baltimore, Maryland, USA

[6]Division of Biostatistics and Bioinformatics, University of Maryland Marlene and Stewart Greenebaum Comprehensive Cancer Center, Baltimore, Maryland, USA

[7]Department of Epidemiology and Public Health, University of Maryland School of Medicine, Baltimore, Maryland, USA

[8]Department of Microbiology and Immunology, University of Maryland Marlene and Stewart Greenebaum Comprehensive Cancer Center, Baltimore, Maryland, USA

[9]Department of Biochemistry and Molecular Biology, University of Maryland School of Medicine, Baltimore, Maryland, USA

[10]Marlene and Stewart Greenebaum Comprehensive Cancer Center, University of Maryland School of Medicine, Baltimore, Maryland, USA

Correspondence
Vincent C. O. Njar, Department of Pharmacology, University of Maryland School of Medicine, 685 West Baltimore St, Baltimore, MD 21201, USA.
Email: vnjar@som.umaryland.edu

Abstract

Cancer stem cells (CSCs) virtually present in all tumors albeit in small numbers are primarily responsible for driving cancer progression, metastasis, drug resistance, and recurrence. Prostate cancer (PCa) is the second most frequent cancer in men worldwide, and castration resistant prostate cancer (CRPC) remains a major challenge despite the tremendous advancements in medicine. Currently, none of the available treatment options are effective in treating CRPC. We earlier reported that VNPP433-3β, the lead next-generation galeterone analog is effective in treating preclinical *in vivo* models of CRPC. In this study using RNA-seq, cytological, and biochemical methods, we report that VNPP433-3β inhibits prostate CSCs by targeting key pathways critical to stemness and epithelial–mesenchymal transition.

ABBREVIATIONS: AR, androgen receptor; CSC, cancer stem cell; DHT, dihydrotestosterone; eIF4E, eukaryotic translation initiation factor 4E; EMT, epithelial–mesenchymal transition; fAR, full-length AR; FBS, fetal bovine serum; GSEA, Gene Set Enrichment Analysis; MMP-2, matrix metalloproteinase-2; MMP-9, matrix metalloproteinase-9; MNK1/2 (MKNK1/2), MAP kinase-interacting serine/threonine-protein kinase 1 and 2; MTT, 3-(4,5-dimethylthiazol-2-yl)–2,5-diphenyltetrazolium bromide; PCa, prostate cancer; p-eIF4E, phosphorylated eukaryotic translation initiation factor 4E; STAT3, signal transducer and activator of transcription 3.

Elizabeth Thomas and Retheesh S. Thankan contributed equally to this study.

VNPP433-3β inhibits CSCs in PCa, presumably by degrading the androgen receptor (AR) thereby decreasing the AR-mediated transcription of several stem cell markers including BMI1 and KLF4. Transcriptome analyses by RNA-seq, Ingenuity Pathway Analysis, and Gene Set Enrichment Analysis demonstrate that VNPP433-3β inhibits transcription of several genes and functional pathways critical to the prostate CSCs thereby inhibiting CSCs in PCa besides targeting the bulk of the tumor.

1 | INTRODUCTION

Pluripotent stem cells are undifferentiated "ever-young" cells capable of self-renewal and differentiation into any type of mature cell in the body. Comparably, cancer stem cells (CSCs) constitute a small subgroup of cells within the tumor and exhibit the features of pluripotent stem cells. CSCs undergo active cell division or may remain quiescent until activated by appropriate stimuli. They are extremely tumorigenic in xenograft models of different cancers and as little as 100 cells could initiate tumor growth whereas tens of thousands of other types of cancer cells of same origin failed to induce tumor.[1] CSCs can be distinguished from other cells within the tumor by symmetry of their cell division and alterations in their gene expression. A variety of cell surface markers (CD24, CD44, CD133, CD166, EpCAM, etc.) and intracellular markers (BMI1, Oct3/4, Nanog, Sox2, etc.) are used to identify and isolate CSCs.[2] In general, tumor consists of heterogenous population of cells often with hierarchical organization that reflects the hierarchy in the tissue of origin and driven by small number of CSCs. However, the bulk of the tumor is comprised of non-CSCs with limited proliferation potential and hence restricted role in long-term growth. However, tumor provides specialized micro niches to haven typically quiescent CSCs that play significant role in unceasing tumor growth, metastasis, relapse, and drug resistance.[3] CSCs are pivotal in epithelial-to-mesenchymal transition, thereby significantly contributing to tumor invasion and metastasis. In fact, several studies have shown that overexpression of epithelial–mesenchymal transition (EMT) transcription factors not only promoted EMT but also invoked stemness and enhanced the tumorigenic potential of cell lines.[4–6] Further, it is reported that the residual population of chemotherapy-resistant tumor cells that can relapse tumor is enriched in CSCs. The intrinsic property of normal stem cells and CSCs such as the upregulation of drug-efflux pumps, enhanced DNA-repair activity and protection against ROS, and the ability of CSCs to assume a quiescent state have emerged as key mechanism of drug resistance and survival.[1]

Prostate cancer (PCa) ranks the second most frequently diagnosed cancer in men worldwide and cancer-related death in the United States.[7] Androgen deprivation therapy is the first-line treatment in the early stage of the disease but inevitably PCa progresses to castration resistant prostate cancer (CRPC), predominantly driven by residual androgen receptor (AR) signaling.[8] Clinically, CRPC is the advanced stage of the disease, which is no longer responsive to available treatment regimens. CSCs play significant role in all stages of PCa, namely tumor initiation, progression, metastasis, and most remarkably, development of CRPC and tumor recurrence.[9] Previously, we reported VNPP433-3β, the lead next generation galeterone analog as potential drug in treating castration-resistant drug-naive PCa preclinical mice models *in vitro* and *in vivo*.[10] VNPP433-3β promotes degradation of AR and its splice variant AR-V7 besides depleting MNk1/2 in PCa.[11]

In this study, we report isolation of CSCs from LNCaP (androgen-dependent human prostate adenocarcinoma cells) and CWR22Rv1 (castration resistant, androgen-independent human prostate cancer cell line) and demonstrate the inhibitory effect of VNPP433-3β in prostate CSCs using cellular, biochemical, and molecular (RNA-seq) methods. We demonstrate that mechanistically, VNPP433-3β promotes degradation of AR thereby limiting AR-mediated transcription of several genes relevant to cell cycle and stemness (*viz.* BMI1 and KLF4). Concurrently, VNPP433-3β also promotes degradation of MNK1/2 thereby interfering with both androgen signaling and MNK1/2-eIF4E signaling. Using RNA-seq followed by Gene Ontology (GO), Gene Set Enrichment Analysis (GSEA), and Qiagen Ingenuity Pathway Analysis (IPA), we demonstrate that several genes and functional pathways of cell cycle control and stemness are modulated by VNPP433-3β thereby inhibiting CSCs in prostate cancer besides targeting the bulk of the tumor.

2 | MATERIALS AND METHODS

2.1 | Cell culture and reagents

CWR22Rv1 and LNCaP, the human prostate cancer cell lines, were obtained from ATCC and cultured in RPMI-1640 enriched with 10%

heat-inactivated fetal bovine serum (FBS; GIBCO) and 1% Pen-Strep (10,000 U/ml; Life Technologies) under standard conditions of 37°C and 5% CO_2. The monolayer adherent cultures were maintained in RPMI1640 supplemented with 10% FBS and 1% Pen-Strep at about 80% confluency under standard culture conditions and culture medium replaced every 48 h.

2.2 | Induction of prostasphere

Prostaspheres were induced in PCa cell lines as described previously.[12] Nonadherent sphere (prostasphere) cultures were induced and maintained in six-well ultra-low attachment culture plates (Corning) containing EpiGRO human Prostate Complete Media (Millipore) supplemented with 20 ng/µl hEGF (Gibco), 20 ng/µl bFGF (Gibco), and 1% Pen-Strep. Monolayer parental and prostasphere cultures were propagated for 15 days and subsequently dissociated into single cells using 0.05% trypsin-EDTA solution (Gibco) or StemPro Accutase (Gibco), respectively, before flow cytometry (fluorescence-activated single cell sorting [FACS]). Micrographs of both monolayer and prostasphere cultures were captured using a phase contrast microscope.

2.3 | Immunofluorescent labeling, FACS analysis, and cell sorting

The dissociated cells were immuno-labeled using two fluorescent monoclonal antibodies: Anti-Human CD133/2 (Miltenyi Biotec) and Anti-Human CD44 (BioLegend) following manufacturer's instructions. Flow cytometry analysis was performed in BD FACSAria II using the software package BD FACSDiva 8.0.2. Unstained cells of adherent and suspension cultures were used as control. All experiments were carried out independently three times. Following cell sorting, the double positive CD133$^+$/CD44$^+$ cells were collected and cultured in adherent plates containing the same medium used for induction and maintenance of prostasphere. Subsequently, VNPP433-3β was evaluated for its effect on cell viability, colony formation, and invasion potential of the cultured CSCs. VNPP433-3β was synthesized in-house as described previously and dissolved in cell culture-grade dimethyl sulfoxide (DMSO).

2.4 | Western blotting

The cultured cells were collected by centrifugation and lysed with radioimmunoprecipitation assay buffer containing 1× protease inhibitors cocktail (Roche), 1× phosphatase inhibitors (Thermo Scientific), 1 mmol/L EDTA, and 1 mmol/L phenylmethylsulfonyl fluoride.[13] The cell lysates were subjected to SDS-PAGE and immunoblotted as described previously.[14] All primary antibodies, namely human AR, MNK1, eukaryotic translation initiation factor 4E (eIF4E), phosphorylated eIF4E (p-eIF4E), β-actin, GAPDH, α-tubulin, CD133, Nanog, Sox2, CD44, KLF4, Oct4, BMI1, N-cadherin, β-catenin, c-myc, matrix

metalloproteinase-9 (MMP-9), MMP-2, Twist, and secondary HRP-conjugated anti-rabbit and anti-mouse antibodies used in the study were obtained from Cell Signaling Technology. All other fine chemicals and reagents were purchased from Sigma Aldrich. Plasmid vector that overexpresses full-length AR (fAR) was purchased from OriGene Technologies Inc.

2.5 | RNA-seq and transcriptome analyses

Total RNA was isolated from CWR22Rv1 cells treated with 10 µM VNPP433-3β (24 h) using RNeasy Plus mini kit (Qiagen) following manufacturer's instructions. DMSO vehicle control and drug treatment were performed in triplicates and all RNA samples were quantified and quality-checked using Agilent 2100 Bioanalyzer. Only RNA preps having an RNA Integrity Number (RIN) of 8 or above were considered for RNA-seq experiments. NEB Ultra II Directional RNA library prep kit was used for preparing RNA-Seq libraries. The libraries thus generated were evaluated for size distribution and yield using Qubit and Agilent 2100 Bioanalyzer. RNA sequencing was conducted on Illumina NovaSeq S2 PE100 bp lane at Maryland Genomics, Institute for Genome Sciences, University of Maryland, Baltimore. The quality of sequencing was measured by Phred quality score (Q score) and more than 90% of the sequencing reads attained Q30 (99.9% base call accuracy). GO and GSEA were carried out using GSEA v4.2.2 against Molecular Signatures Database v7.5.1 with permutation set at "gene set" and other parameters default.[15] Qiagen IPA was carried out to uncover canonical pathways modulated by VNPP433-3β.

2.6 | Cell proliferation, colony formation, and invasion assays

The cell proliferation (MTT), colony formation, and invasion assays were performed as described previously.[16] In brief, 2500 CD133$^+$/CD44$^+$ cells were seeded per well in 96-well plates and treated with VNPP433-3β or DMSO vehicle control for second and fifth day for a period of 8 days. GraphPad prism 5.0 software was used to calculate growth inhibitory concentration (GI$_{50}$) based on a nonlinear regression curve fit.[17] Colony formation assay was carried out by seeding 10,000 CD133$^+$/CD44$^+$ cells per well in a six-well adherent plate and treated with VNPP433-3β (5 and 10 µM) twice a week and adherent colony formation was assessed on 15th day using 0.05% (w/v) crystal violet staining solution. Colonies were counted manually and photographed. The invasion assay was performed by seeding 5000 CD133$^+$/CD44$^+$ cells in the top chamber of precoated transwell inserts (corning) in serum-free media. The lower chamber was filled with EpiGro medium and cells were treated with VNPP433-3β (5 and 10 µM) for 24 h. Subsequently, the cells at the upper chamber of the transwell inserts were scraped off with a cotton swab and the migrated cells on the lower surface were fixed with cold methanol, stained with 0.05% (w/v) crystal violet, and photographed.

2.7 | Statistical analysis

Statistical evaluations were carried out using one-way analysis of variance followed by Student's t-test using GraphPad Prism 5.0 software (GraphPad Software Inc.). A probability value with *$p < 0.05$, **$p < 0.01$, and ***$p < 0.001$ were considered statistically significant. The values in the data are presented as mean ± standard error of mean of three or more independent experiments.

3 | RESULTS

3.1 | Degradation of AR and Mnk1/2 by VNPP433-3β

Aberrant androgen signaling is essential for PCa development and progression. Studies showed that activation of AR suppresses eIF4E phosphorylation whereas antagonizing AR with anti-androgens stimulated eIF4E phosphorylation.[18] To evaluate the effect of VNPP433-3β on AR signaling and MNK1/2-mediated phosphorylation of eIF4E, we examined the levels of fAR, its splice-variant AR-V7, eIF4E, p-eIF4E, and its upstream kinase MNK1/MNK2 in CWR22Rv1 and LNCaP cells following treatment with varying concentrations of VNPP433-3β (0.6, 1.25, 2.5, 5, 10, 15, 20 μM) for 48 h (Figure 1A,B). Interestingly, we observed that VNPP433-3β promotes significant degradation of fAR and AR-V7 at 1.25 μM and upwards in CWR22Rv1 and LNCaP cells in a dose-dependent manner. Further, we observed a distinct decrease in the level of MNK1/2 with concomitant decline of p-eIF4E in a dose-dependent manner. Our results demonstrate that VNPP433-3β promotes degradation of AR thus inhibiting the cellular AR response and depletes MNK1/2 thereby preventing eIF4E phosphorylation crucial for inhibiting PCa and prostate CSCs as described below.

3.2 | CSC-enriched prostaspheres show upregulation of stem cell markers

Further, we induced the formation of prostaspheres enriched in CSCs in CWR22Rv1 and LNCaP cell lines. Figure 2A–D shows the phase contrast micrographs and flow cytometry scatter-plots of control monolayer cultures of CWR22Rv1 and LNCaP and corresponding prostasphere cultures enriched in CSCs. The CSCs were analyzed and sorted using FACS following immunolabeling with fluorescent monoclonal antibodies specific to stem cell surface markers CD44 and CD133. Only the cells displaying both markers on the surface were considered CSCs and were sorted and cultured further for additional experiments. We found that the monolayer cultures of CWR22Rv1 and LNCaP possessed 0.10 ± 0.005% and 0.15 ± 0.029% CD44+/CD133+ cells, respectively, whereas the cultured prostaspheres were significantly enriched with CSCs, 4.850 ± 1.05% and 2.725 ± 0.24%, respectively (Figure 2E).

Several studies report that CSCs heavily rely on active electron transport and oxidative phosphorylation (OXPHOS) though aerobic glycolysis is a key metabolic adaptation of cancer cells.[19–21] Greater dependency of tumor on OXPHOS is often a hallmark of CSCs and pharmacologically targeting OXPHOS is a rational approach to treat various cancers.[22,23] It was reported that the relapsing tumors were susceptible to treatment with oligomycin, a potent OXPHOS inhibitor.[24] Moreover, apart from the canonical role of mitotic spindle in chromosome segregation during cell division, it plays critical role in determining cleavage plane and self-renewal associated with stem cells.[25] The GSEA plots of RNA-seq shows that VNPP433-3β significantly inhibited OXPHOS and mitotic spindle characteristic to CSCs (Figure 2F,G). Further, these prostaspheres were analyzed for stem cell markers by immunoblotting and found that the levels of KLF4, CD44, Oct4, BMI1, Nanog, Sox2, and CD133 were enhanced in prostasphere cultures compared to the monolayer controls (Figure 2H,I). However, the levels of these proteins were significantly decreased in CSCs when treated with 5 and 10 μM VNPP433-3β in a concentration-dependent manner.

3.3 | Knockdown of AR leads to decreased levels of EMT markers

We next explored the effect of small interfering RNA (siRNA)-mediated knockdown of AR on EMT markers as several reports implicate AR in EMT and metastasis of PCa, apparently led by CSCs.[23,26] Whereas
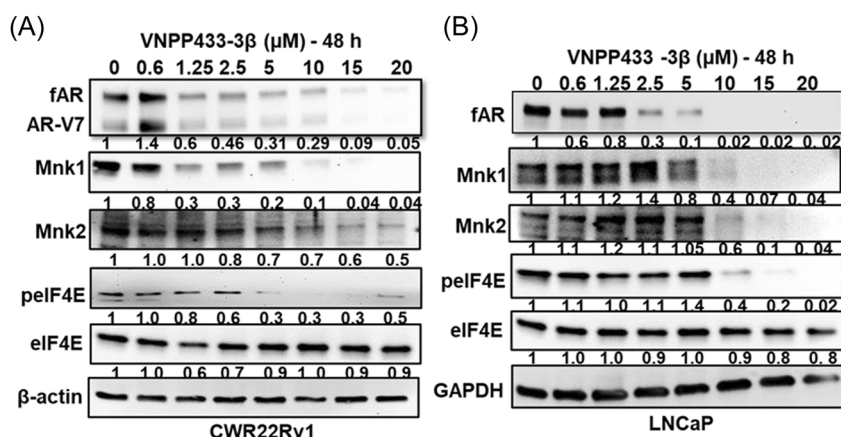

FIGURE 1 VNPP433-3β promotes degradation of AR and Mnk1/2 and decreases the level of p-eIF4E. (A) and (B) Immunoblots of fAR, AR-V7, Mnk1, Mnk2, eIF4E, p-eIF4E following treatment with varying concentrations of VNPP433-3β in CWR22Rv1 and LNCaP cells. GAPDH or β-actin served as loading control. AR, androgen receptor; eIF4E, eukaryotic translation initiation factor 4E; p-eIF4E, phosphorylated eIF4E.
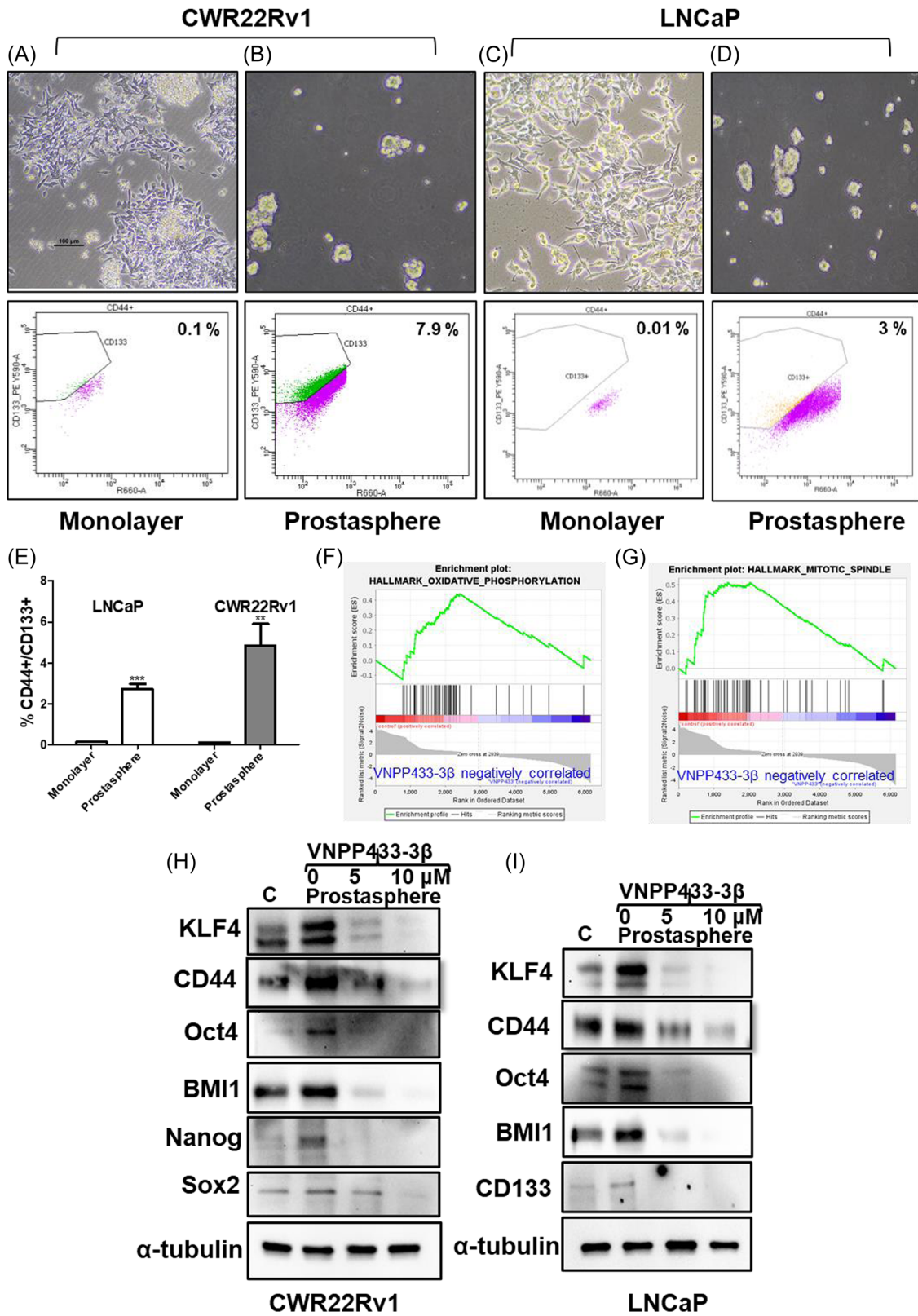
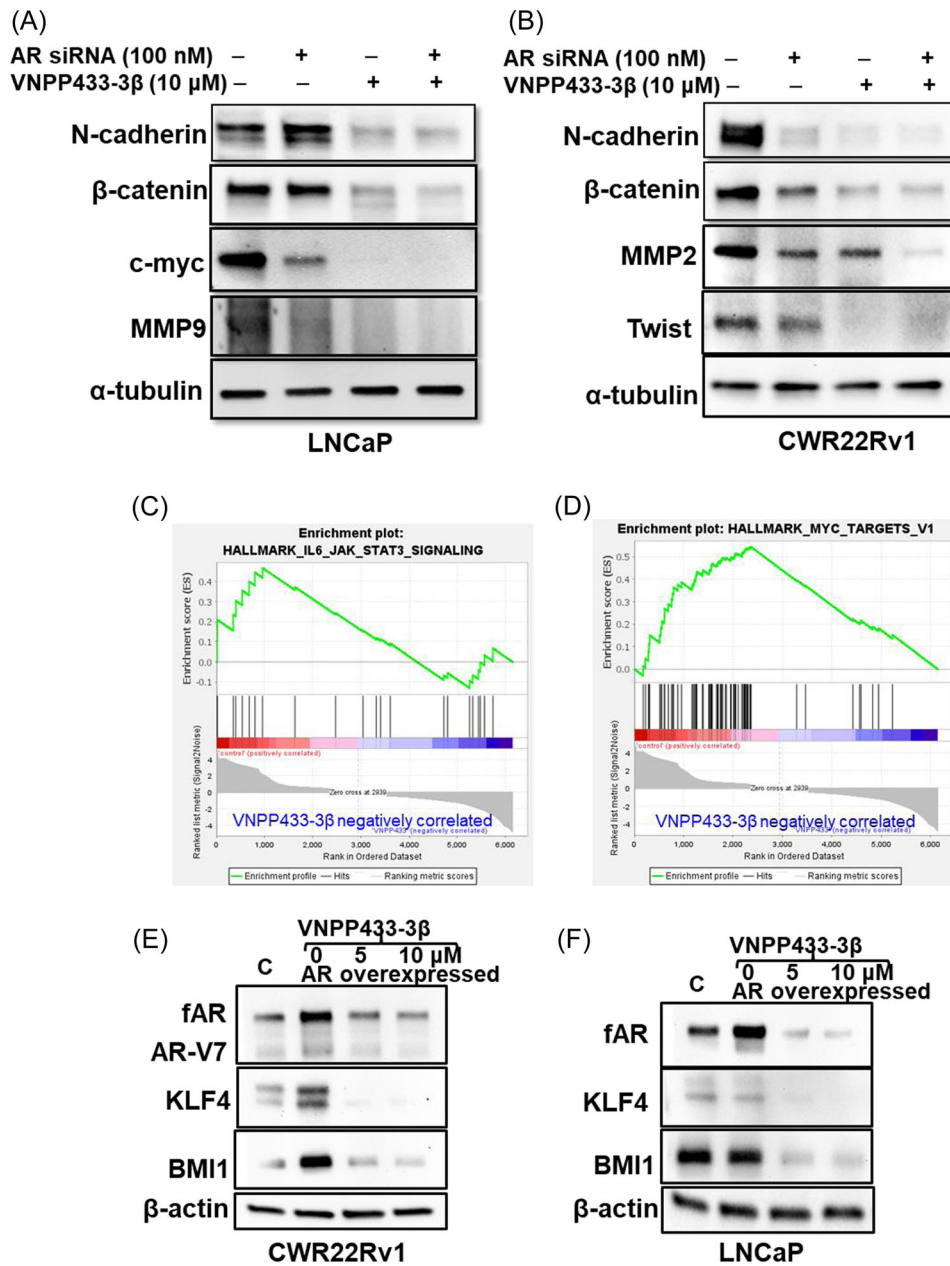**FIGURE 2** (See caption on next page)

FIGURE 3 Knockdown of AR leads to decreased levels of EMT markers. (A) and (B) siRNA-mediated knockdown of AR decreased the level of EMT markers in CWR22Rv1 and LNCaP cells. (C) and (D) GSEA plots showing VNPP433-3β-mediated inhibition of two pathways (IL-6-JAK-STAT3 signaling and Myc targets) critical to CSCs in CWR22Rv1 cells. (E) and (F) AR is transcriptional activator of BMI1 and KLF4. Overexpression of full-length AR leads to increased expression of stem cell markers BMI1 and KLF4, but treatment with VNPP433-3β revoked this effect by degrading AR and thereby decreasing the levels of BMI1 and KLF4 in CWR22Rv1 and LNCaP cells. AR, androgen receptor; CSC, cancer stem cell; EMT, epithelial–mesenchymal transition; GSEA, Gene Set Enrichment Analysis; IL-6, interleukin 6; siRNA, small interfering RNA; STAT3, signal transducer and activator of transcription 3 [Color figure can be viewed at wileyonlinelibrary.com]

FIGURE 2 Induction of prostaspheres enriched in CSCs (CD44$^+$/CD133$^+$) in PCa cell lines. (A–D) Phase contrast micrographs and flow cytometry scatter plots of CWR22Rv1 and LNCaP parental monolayer adherent culture and prostasphere suspension culture enriched in CSCs. The adherent monolayer culture was photographed at fourth day of culture and consisted of cells with typical epithelial morphology and prostasphere suspension cultures were photographed at 12th day of induction and consisted of spherical to irregular clusters. Flow cytometric analysis of monolayer culture and corresponding prostasphere culture (single cell suspension) enriched in CSCs that are positive for CD44 and CD133: the single cell suspensions were labeled with fluorescently labeled CD44 and CD133 monoclonal antibodies. (E) The yield of CD44$^+$/CD133$^+$ CSCs in culture is presented in the graph. $p = 0.0041$ (CWR22Rv1), $p < 0.0001$ (LNCaP). (F) and (G) GSEA plots of RNA-seq show that VNPP433-3β inhibited OXPHOS and mitotic spindle pathways critical to CSCs. (H) and (I) Immunoblots demonstrating the prostaspheres enriched in CSCs expressed higher levels of EMT markers than the adherent monolayer culture, but treatment with VNPP433-3β significantly decreased the EMT markers in CWR22Rv1 and LNCaP prostaspheres. CSC, cancer stem cell; EMT, epithelial–mesenchymal transition; GSEA, Gene Set Enrichment Analysis; OXPHOS, oxidative phosphorylation; PCa, prostate cancer [Color figure can be viewed at wileyonlinelibrary.com]
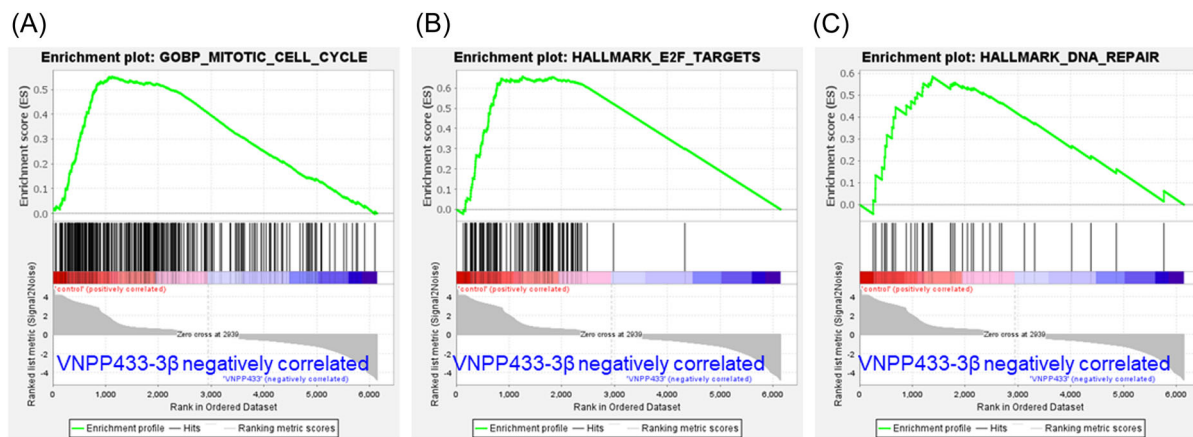
FIGURE 4 Functional pathways important to CSCs are modulated by VNPP433-3β. GSEA plots showing VNPP433-3β-mediated inhibition of three pathways critical to CSCs and prostate cancer progression: mitotic cell cycle (A), E2F signaling (B), and DNA repair (C). CSC, cancer stem cell; GSEA, Gene Set Enrichment Analysis [Color figure can be viewed at wileyonlinelibrary.com]

another study reports that AR played negative role in EMT of PCa stem progenitor cells[27] probably due to the feedback loop that involves AR and Zeb1.[28] Interestingly, we observed that siRNA knockdown of AR led to decrease in the levels of many EMT markers such as N-cadherin, β-catenin, MMP-2, MMP-9, and Twist reflecting the effect of VNPP433-3β per se (Figure 3A,B). EMT markers play significant role in EMT and cancer cell stemness.[26] CSCs are shown to rely on interleukin 6 (IL-6)-JAK-signal transducer and activator of transcription 3 (STAT3) signaling in different cancers. Earlier reports suggest that IL-6 activates Notch 3 and promotes self-renewal of CSCs.[29] IL-6 inhibition decreased the fraction of CSCs and averts tumor recurrence.[30] Similarly, activation of STAT3 signaling promotes glioblastoma stem cells,[31] urothelial stem cells,[32] and colorectal CSCs.[33] However, treatment with 10 μM VNPP433-3β for 24 h significantly inhibited IL-6-JAK-STAT3 signaling (Figure 3C). Earlier reports suggests that AR promotes PCa by upregulating the expression of c-Myc.[34] In our study, we noted a decrease in c-Myc protein upon siRNA knockdown of AR and VNPP433-3β-mediated degradation of AR (Figure 3A). Similar response is obtained in RNA-seq experiment where the GSEA plot shows a significant inhibition of c-Myc targets (Figure 3D). Since c-Myc is central to transcriptionally activating several oncogenic pathways including stemness,[35] decrease in its level further contributes to inhibition of CSCs and PCa itself. Besides many other factors, BMI1 and KLF4 oncoproteins that are transcriptionally regulated by AR are two key proteins responsible for EMT and stemness in CSCs.[36,37] As expected, overexpression of fAR led to increased expression of stem cell markers BMI1 and KLF4, but treatment with VNPP433-3β revoked this effect and reduced the levels of AR and its transcriptional targets BMI1 and KLF4 (Figure 3E,F).

3.4 | Functional pathways important to CSCs are modulated by VNPP433-3β

Qiagen IPA of the RNA-seq data reveal that VNPP433-3β (10 μM, 24 h) inhibited human embryonic and pluripotent stem cell pathway besides several other pathways related to cell cycle control and apoptosis in CWR22Rv1 cells. Among the key pathways modulated by VNPP433-3β are cell cycle control of chromosomal replication, S-phase entry, EMT, STAT3 pathway and activation of autophagy, G1-S checkpoint regulation, and p53 signaling. Further, the GSEA of the RNA-seq data shows that VNPP433-3β significantly impaired DNA repair, E2F signaling, and mitotic cell cycle that are necessary for stemness, thus inhibiting the CSCs in PCa (Figure 4A–C).

3.5 | Effect of VNPP433-3β on prostate CSCs

Next, we cultured the FACS-sorted double positive (CD44$^+$/CD133$^+$) CSCs in adherent plate for the evaluation of GI$_{50}$ of VNPP433-3β in CWR22Rv1 and LNCaP stem cells by MTT assay and found that VNPP433-3β exhibited GI$_{50}$ of 0.36 and 0.38 μM in CWR22Rv1 and LNCaP CSCs, respectively (Figure 5A). Further, the colony formation ability that reflects the metastatic potential of FACS-sorted CSCs was studied in presence of VNPP433-3β (Figure 5B). Interestingly, 78% and 55% reduction in colony forming unit (cfu) in both the cell lines was noted when treated with VNPP433-3β at concentration as low as 5 μM for 24 h. Less than 94% and 75% of the cells formed cfu at 10 μM concentration of VNPP433-3β (Figure 5C,D). We observed that the VNPP433-3β treatment substantially inhibited cell invasion of CSCs across the membrane (Figure 5E). Virtually, 75% reduction in invasion compared to the control was detected when CSCs were treated with 10 μM VNPP433-3β for 24 h in CWR22Rv1 and LNCaP whereas only 57% and 27% inhibition was noted at 5 μM (Figure 5F,G). This finding further complements the results of immunoblotting wherein VNPP433-3β decreased the levels of EMT markers in CSCs (Figure 2). The GSEA plots show that VNPP433-3β significantly inhibited EMT and enhanced tumor necrosis factor-α signaling, thereby invoking apoptosis (Figure 5H,I). Overall, the data suggest that the decrease in invasion is due to the VNPP433-3β-induced inhibition of EMT pathway.
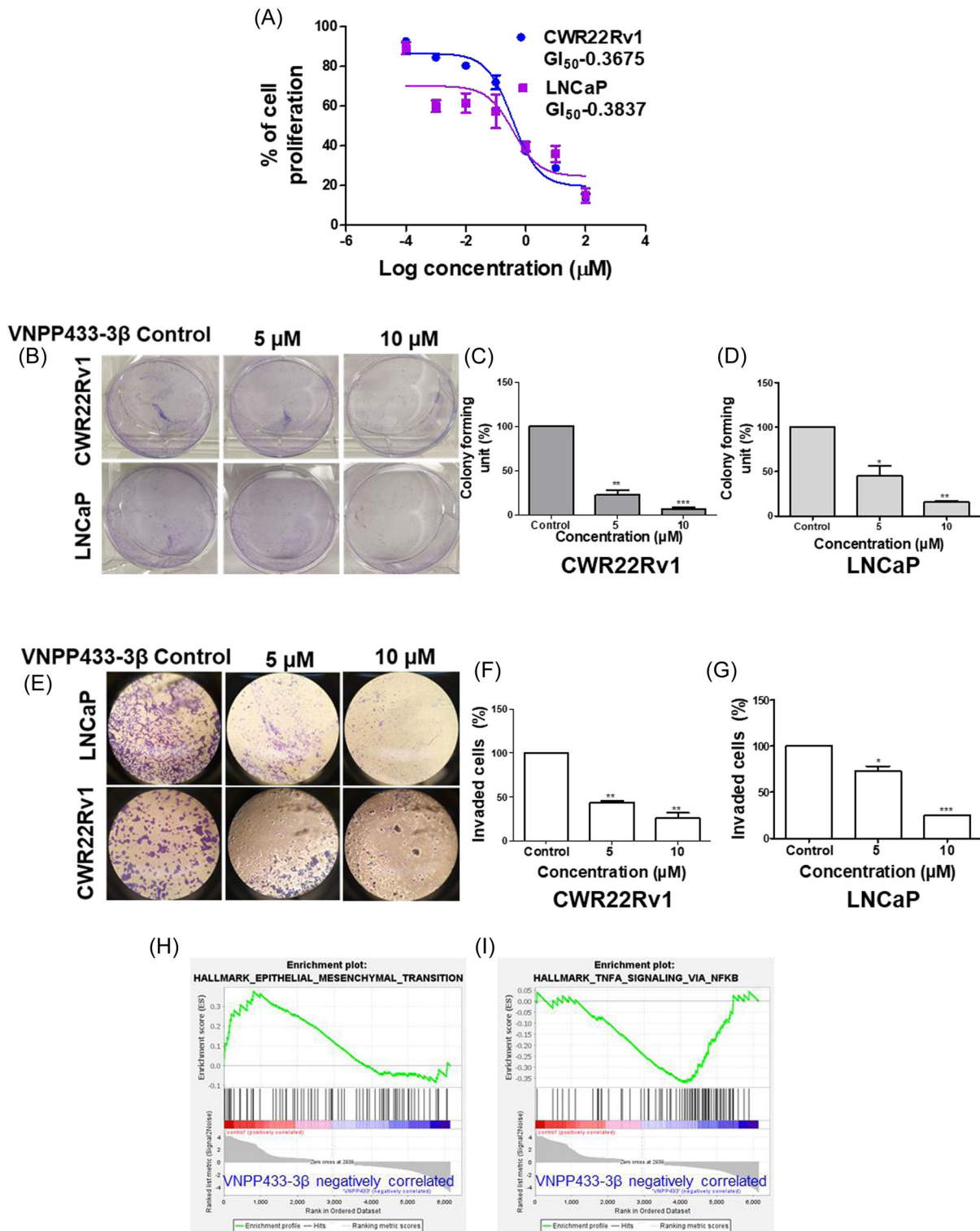
FIGURE 5 Effect of VNPP433-3β on cell viability and invasion potential of FACS-sorted PCa CSCs. (A) cell viability as determined by MTT assay, (B–D) Effect of VNPP433-3β in colony formation, and (E–G) invasion of CWR22Rv1 and LNCaP CSCs (CD44⁺/CD133⁺) were assessed. Graphs show the standard error of mean and *p*-value of the colonies within three independent treatment groups as compared to that of vehicle controls, *p< 0.05, **p < 0.005, ***p < 0.0001. The cells were stained with crystal violet and plates were photographed. (H) GSEA plot demonstrating inhibition of epithelial–mesenchymal transition (EMT) thus inhibiting cell invasion. (I) RNA-seq GSEA plot showing activation of TNFA signaling by VNPP433-3β, thereby inhibiting cell proliferation and colony formation. CSC, cancer stem cell; GSEA, Gene Set Enrichment Analysis; PCa, prostate cancer [Color figure can be viewed at wileyonlinelibrary.com]
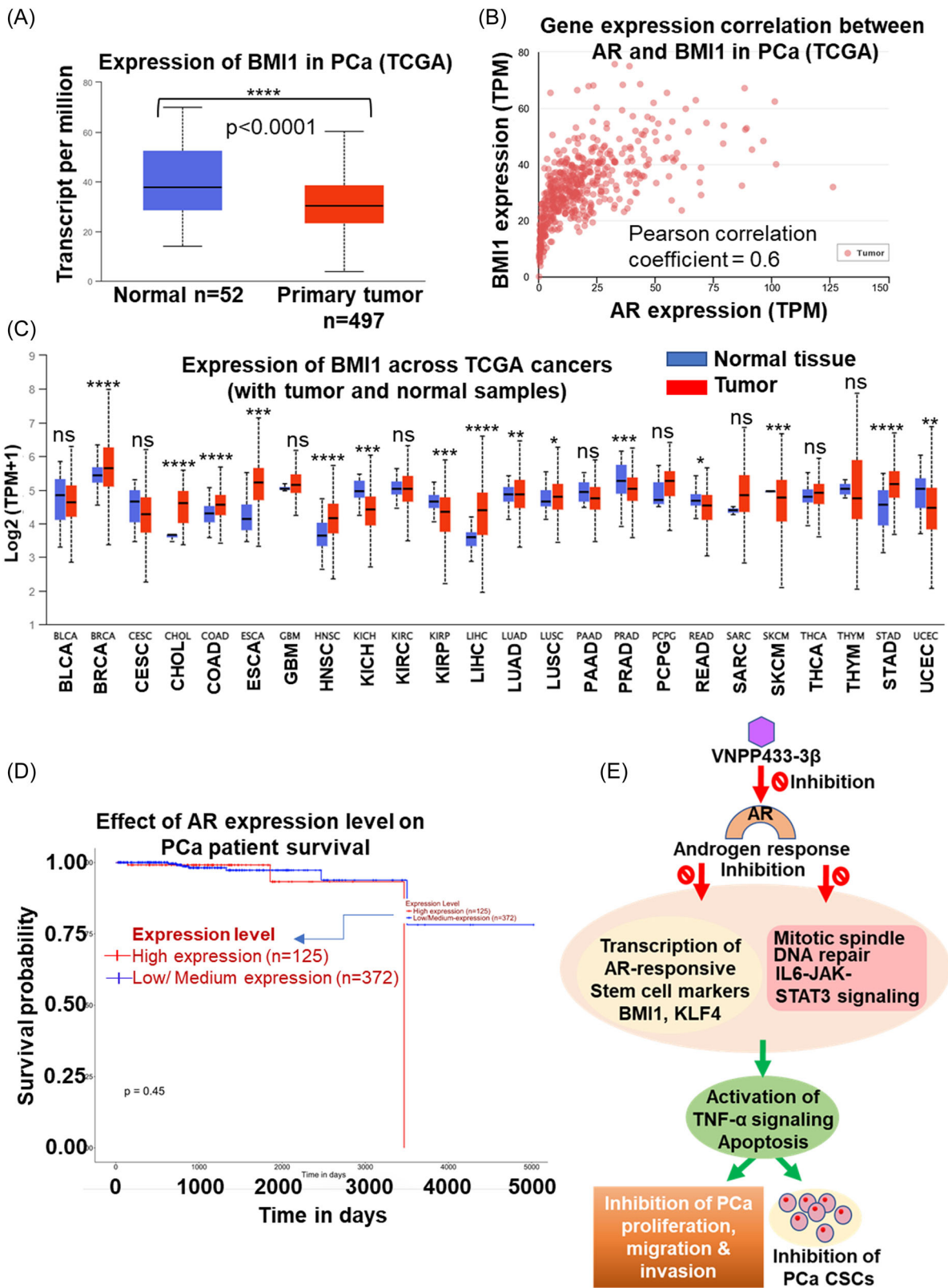
(A)

Expression of BMI1 in PCa (TCGA)

(B)

Gene expression correlation between AR and BMI1 in PCa (TCGA)

(C)

Expression of BMI1 across TCGA cancers (with tumor and normal samples)

(D)

Effect of AR expression level on PCa patient survival

(E)

FIGURE 6 (See caption on next page)

4 | DISCUSSION

AR is known to activate transcription of key stem cell markers KLF4 and BMI1 by directly binding to its promoter.[36,37] AR being a central transcription factor, besides enhancing KLF4 expression, it enhances the transcription of BMI1 and promote castration-resistance in prostate cancer.[36] BMI1 is recognized for its prominent role in tumorigenesis by repressing the transcription of tumor suppressor proteins. The expression of AR and BMI1 is positively correlated as dihydrotestosterone (DHT) elicits increase in BMI1 RNA and protein, presumably due to the increased AR activity triggered by DHT. Presence of AR binding site in the BMI1 promoter is established and elevated levels of BMI1 RNA and protein are recorded in human CRPC patients and mice xenograft models.[36] The Cancer Genome Atlas (TCGA) data show that AR and BMI1 are misregulated in prostate cancer (Figure 6A–C) and BMI1 is upregulated in most of the TCGA cancers (Figure 6C). The levels of AR and BMI1 are positively correlated in prostate cancer patients (Figure 6B). The overall survival of patients expressing AR is significantly reduced compared to the low-level AR groups (Figure 6D). In our study, overexpression of AR protein increased the protein levels of BMI1 and KLF4 in LNCaP and CWR22Rv1 cell lines, emphasizing the role of AR-regulated BMI1 and KLF4 in stemness of PCa. However, treating with VNPP433-3β significantly impaired the androgen response presumably by degrading AR and thereby inhibiting several pathways associated with stemness and cell proliferation.

Orientation of mitotic spindle is a determinant feature of stem cells. Apart from the canonical role of mitotic spindle in chromosome segregation during cell division, it plays critical role in determining cleavage plane. Asymmetric cell division of stem cells and the correlation between positioning of cleavage plane and cell-fate choice as defined by mitotic spindle orientation has been well recognized.[38,39] Parallel cleavage plane results in placing each daughter cell at the apical and basal surface whereas a perpendicular cleavage generates daughter cells that inherit equal amounts of apical and basal membrane.[25] Interestingly, VNPP433-3β significantly downregulated formation of mitotic spindle, a prerequisite to halt cell division featured in CSCs, and the rest of the tumor cells.

Significantly, VNPP433-3β treatment is associated with negative regulation of Myc signaling and OXPHOS. Myc signaling is crucial for normal embryogenesis and acquisition and maintenance of stemness by cancer cells.[35] c-Myc is known to promote dedifferentiation by downregulating lineage-specifying transcriptional factors and therefore c-Myc-induced oncogenic and epigenetic reprogramming leads to the acquisition of cancer stem-like properties resulting in CSCs.[35,40,41] In various clinical cases, c-Myc- or N-Myc-driven tumors are found to result from cell lineages that express a given variant during the normal development of each tissue. Often, N-Myc is expressed in self-renewing, quiescent stem cells, but it switches to c-Myc upon differentiation.[42] In prostate cancer, increasing reports suggests that N-Myc is crucial in lineage switching from epithelial origin to neuroendocrine lineage. Switching of expression among Myc family during tumor growth may be correlated to tumor progression and treatment resistance.[35,42]

Adaptation of cancer cells to aerobic glycolysis does not warrant complete shutdown OXPHOS pathway as reports demonstrate that active electron transport occurs in cancer cells that facilitate tumor recurrence and CSCs.[19–21] Though aerobic glycolysis is a key metabolic adaptation of cancer cells, growing evidence suggest that OXPHOS plays a critical role in meeting the energy demand in high grade serous ovarian cancer, especially the CSCs.[43] Further, it was reported that the relapsing tumors were susceptible to treatment with oligomycin, a potent OXPHOS inhibitor.[24] It is demonstrated that the key objective of OXPHOS in tumors is to support the survival and proliferation of CSCs. The tumor initiating cells of murine ovarian surface epithelial cells expressed higher levels of glucose transporters with increased rate of glycolysis besides having increased mitochondrial oxygen consumption.[44] Studies show that CD44+/CD117+ CSCs in mice generated higher levels of oxygen radicals and had enhanced OXPHOS than the nonstem cell (CD44+/CD117−) population. In RAG2−/− mice bearing HGSOC tumors and fed with 2-deoxyglucose, a glycolysis inhibitor, the tumor size was decreased but the surviving tumor cells were enriched in CD44+/CD117+ CSCs, which strongly suggest the role of OXPHOS in survival and proliferation of CSCs.[19] A generic scheme of effect of VNPP433-3β on PCa[22] CSCs is presented in Figure 6E. Taken together, the cytological, biochemical, and molecular data suggest that VNPP433-3β inhibits prostate CSCs besides targeting the bulk of the tumor.

FIGURE 6 TCGA data showing significance of AR and AR-regulated stem cell marker BMI1 in prostate cancer and other TCGA cancers. (A) BMI1 is aberrantly expressed in prostate cancer patients (n = 497) compared to normal prostate tissue (n = 52). (B) Expression of BMI1 is positively correlated to the expression of AR in prostate cancer patients. (C) BMI1 is overexpressed in most of the TCGA cancers compared to the normal tissue (p > 0.1 ns, *p < 0.05, **p < 0.01, ***p < 0.001, ****p < 0.0001). (D) The overall survival of prostate cancer patients was negatively related to the level of AR expression. Over 90% patients with high AR expression survived not more than 3500 days but 75% of PCa patients with medium or low levels of AR registered survival beyond 5000 days. (E) A generic scheme of effect of VNPP433-3β on PCa CSCs. VNPP433-3β degrades AR and decreases AR-dependent transcription of stem cell factors BMI1, KLF4 besides inhibiting EMT, mitotic spindle, DNA repair, IL-6-JAK-STAT3, and Myc signaling but activating apoptosis and TNF-α signaling thereby inhibiting CSCs and other tumor cells. AR, androgen receptor; CSC, cancer stem cell; EMT, epithelial–mesenchymal transition; GSEA, Gene Set Enrichment Analysis; IL-6, interleukin 6; PCa, prostate cancer; STAT3, signal transducer and activator of transcription 3; TCGA, The Cancer Genome Atlas; TNF-α, tumor necrosis factor-α [Color figure can be viewed at wileyonlinelibrary.com]

5 | CONCLUSION

VNPP433-3β inhibits CSCs in prostate cancer, presumably by degrading the AR thereby decreasing the AR-mediated transcription of key stem cell markers BMI1 and KLF4. Transcriptome analyses demonstrate that VNPP433-3β inhibits transcription of several genes and functional pathways critical for prostate CSCs.

AUTHOR CONTRIBUTIONS

The study was conceptualized and designed by Elizabeth Thomas, Retheesh S. Thankan, Puranik Purushottamachar, and Vincent C. O. Njar. Elizabeth Thomas, Retheesh S. Thankan, and Puranik Purushottamachar performed the experiments and acquired data. The data were analyzed by Elizabeth Thomas, Retheesh S. Thankan, Puranik Purushottamachar, Weiliang Huang, Maureen A. Kane, Yuji Zhang, Nicholas Ambulos, David J. Weber, and Vincent C. O. Njar. Elizabeth Thomas, Retheesh S. Thankan, and Vincent C. O. Njar wrote the manuscript. Vincent C. O. Njar supervised the entire study. All authors read and approved the final manuscript.

ACKNOWLEDGMENTS

CONFLICTS OF INTEREST

The authors declare no conflicts of interest.

DATA AVAILABILITY STATEMENT

The data sets used and analyzed during the current study are available from the corresponding author on reasonable request.

REFERENCES

1. Batlle E, Clevers H. Cancer stem cells revisited. *Nat Med*. 2017; 23(10):1124-1134.
2. Walcher L, Kistenmacher AK, Suo H, et al. Cancer stem cells-origins and biomarkers: perspectives for targeted personalized therapies. *Front Immunol*. 2020;11:1280.
3. Desai A, Yan Y, Gerson SL. Concise reviews: cancer stem cell targeted therapies: toward clinical success. *Stem Cells Transl Med*. 2019;8(1):75-81.
4. Mani SA, Guo W, Liao MJ, et al. The epithelial-mesenchymal transition generates cells with properties of stem cells. *Cell*. 2008; 133(4):704-715.
5. Morel AP, Lievre M, Thomas C, Hinkal G, Ansieau S, Puisieux A. Generation of breast cancer stem cells through epithelial-mesenchymal transition. *PLoS One*. 2008;3(8):e2888.
6. Ye X, Tam WL, Shibue T, et al. Distinct EMT programs control normal mammary stem cells and tumour-initiating cells. *Nature*. 2015;525(7568):256-260.
7. Siegel RL, Miller KD, Jemal A. Cancer statistics, 2020. *CA Cancer J Clin*. 2020;70(1):7-30.
8. Watson PA, Arora VK, Sawyers CL. Emerging mechanisms of resistance to androgen receptor inhibitors in prostate cancer. *Nat Rev Cancer*. 2015;15(12):701-711.
9. Mei W, Lin X, Kapoor A, Gu Y, Zhao K, Tang D. The contributions of prostate cancer stem cells in prostate cancer initiation and metastasis. *Cancers (Basel)*. 2019;11(4):434.
10. Kwegyir-Afful AK, Ramalingam S, Ramamurthy VP, et al. Galeterone and the next generation galeterone analogs, VNPP414 and VNPP433-3beta exert potent therapeutic effects in castration-/drug-resistant prostate cancer preclinical models in vitro and in vivo. *Cancers (Basel)*. 2019;11(11):1637.
11. Thomas E, Thankan RS, Purushottamachar P, Njar VC. Mechanistic insights on the effects of the lead next generation galeterone analog, VNPP433-3β in castration resistant prostate cancer. *Mol Cancer Ther*. 2021;20:LBA027.
12. Portillo-Lara R, Alvarez MM. Enrichment of the cancer stem phenotype in sphere cultures of prostate cancer cell lines occurs through activation of developmental pathways mediated by the transcriptional regulator DeltaNp63alpha. *PLoS One*. 2015;10(6): e0130118.
13. Hegde M, Sharathkumar SK, Thomas E, Hanumappa A, Raghavan SC, Rangappa KS. A novel benzimidazole derivative binds to DNA minor groove induces apoptosis in leukemic cells. *RSC Adv*. 2015;5: 93194-93208.
14. Thomas E, Gopalakrishnan V, Hegde M, et al. A novel resveratrol based tubulin inhibitor induces mitotic arrest and activates apoptosis in cancer cells. *Sci Rep*. 2016;6:34653.
15. Subramanian A, Tamayo P, Mootha VK, et al. Gene set enrichment analysis: a knowledge-based approach for interpreting genome-wide expression profiles. *Proc Natl Acad Sci USA*. 2005;102(43): 15545-15550.
16. Thomas E, Gopalakrishnan V, Somasagara RR, Choudhary B, Raghavan SC. Extract of *Vernonia condensata*, inhibits tumor progression and improves survival of tumor-allograft bearing mouse. *Sci Rep*. 2016;6:23255.
17. Hegde M, Karki SS, Thomas E, et al. Novel levamisole derivative induces extrinsic pathway of apoptosis in cancer cells and inhibits tumor progression in mice. *PLoS One*. 2012;7(9):e43632.
18. D'Abronzo LS, Ghosh PM. eIF4E phosphorylation in prostate cancer. *Neoplasia*. 2018;20(6):563-573.
19. Pastò A, Bellio C, Pilotto G, et al. Cancer stem cells from epithelial ovarian cancer patients privilege oxidative phosphorylation, and resist glucose deprivation. *Oncotarget*. 2014;5(12):4305-4319.
20. De Luca A, Fiorillo M, Peiris-Pagès M, et al. Mitochondrial biogenesis is required for the anchorage-independent survival and propagation of stem-like cancer cells. *Oncotarget*. 2015;6(17):14777-14795.
21. Lamb R, Bonuccelli G, Ozsvári B, et al. Mitochondrial mass, a new metabolic biomarker for stem-like cancer cells: understanding WNT/FGF-driven anabolic signaling. *Oncotarget*. 2015;6(31):30453-30471.
22. Xu Y, Xue D, Bankhead A, 3rd, Neamati N. Why all the fuss about oxidative phosphorylation (OXPHOS)? *J Med Chem*. 2020;63(23): 14276-14307.
23. Lin CY, Jan YJ, Kuo LK, et al. Elevation of androgen receptor promotes prostate cancer metastasis by induction of epithelial-mesenchymal transition and reduction of KAT5. *Cancer Sci*. 2018; 109(11):3564-3574.
24. Viale A, Pettazzoni P, Lyssiotis CA, et al. Oncogene ablation-resistant pancreatic cancer cells depend on mitochondrial function. *Nature*. 2014;514(7524):628-632.
25. Gotz M, Huttner WB. The cell biology of neurogenesis. *Nat Rev Mol Cell Biol*. 2005;6(10):777-788.
26. Zhu ML, Kyprianou N. Role of androgens and the androgen receptor in epithelial-mesenchymal transition and invasion of prostate cancer cells. *FASEB J*. 2010;24(3):769-777.
27. Zhifang M, Liang W, Wei Z, et al. The androgen receptor plays a suppressive role in epithelial-mesenchymal transition of human prostate cancer stem progenitor cells. *BMC Biochem*. 2015;16:13.

28. Sun Y, Wang BE, Leong KG, et al. Androgen deprivation causes epithelial-mesenchymal transition in the prostate: implications for androgen-deprivation therapy. *Cancer Res*. 2012;72(2):527-536.

29. Sansone P, Storci G, Tavolari S, et al. IL-6 triggers malignant features in mammospheres from human ductal breast carcinoma and normal mammary gland. *J Clin Invest*. 2007;117(12):3988-4002.

30. Finkel KA, Warner KA, Kerk S, et al. IL-6 inhibition with MEDI5117 decreases the fraction of head and neck cancer stem cells and prevents tumor recurrence. *Neoplasia*. 2016;18(5): 273-281.

31. Kim E, Kim M, Woo DH, et al. Phosphorylation of EZH2 activates STAT3 signaling via STAT3 methylation and promotes tumorigenicity of glioblastoma stem-like cells. *Cancer Cell*. 2013;23(6):839-852.

32. Ho PL, Lay EJ, Jian W, Parra D, Chan KS. Stat3 activation in urothelial stem cells leads to direct progression to invasive bladder cancer. *Cancer Res*. 2012;72(13):3135-3142.

33. Kryczek I, Lin Y, Nagarsheth N, et al. IL-22(+)CD4(+) T cells promote colorectal cancer stemness via STAT3 transcription factor activation and induction of the methyltransferase DOT1L. *Immunity*. 2014; 40(5):772-784.

34. Gao L, Schwartzman J, Gibbs A, et al. Androgen receptor promotes ligand-independent prostate cancer progression through c-Myc upregulation. *PLoS One*. 2013;8(5):e63563.

35. Yoshida GJ. Emerging roles of Myc in stem cell biology and novel tumor therapies. *J Exp Clin Cancer Res*. 2018;37(1):173.

36. Zhu S, Zhao D, Li C, et al. BMI1 is directly regulated by androgen receptor to promote castration-resistance in prostate cancer. *Oncogene*. 2020;39(1):17-29.

37. Mimoto R, Imawari Y, Hirooka S, Takeyama H, Yoshida K. Impairment of DYRK2 augments stem-like traits by promoting KLF4 expression in breast cancer. *Oncogene*. 2017;36(13):1862-1872.

38. Berika M, Elgayyar ME, El-Hashash AH. Asymmetric cell division of stem cells in the lung and other systems. *Front Cell Dev Biol*. 2014; 2:33.

39. Chenn A, McConnell SK. Cleavage orientation and the asymmetric inheritance of Notch1 immunoreactivity in mammalian neurogenesis. *Cell*. 1995;82(4):631-641.

40. Poli V, Fagnocchi L, Fasciani A, et al. MYC-driven epigenetic reprogramming favors the onset of tumorigenesis by inducing a stem cell-like state. *Nat Commun*. 2018;9(1):1024.

41. Fagnocchi L, Poli V, Zippo A. Enhancer reprogramming in tumor progression: a new route towards cancer cell plasticity. *Cell Mol Life Sci*. 2018;75(14):2537-2555.

42. Rickman DS, Beltran H, Demichelis F, Rubin MA. Biology and evolution of poorly differentiated neuroendocrine tumors. *Nat Med*. 2017;23(6):1-10.

43. Nayak AP, Kapur A, Barroilhet L, Patankar MS. Oxidative phosphorylation: a target for novel therapeutic strategies against ovarian cancer. *Cancers (Basel)*. 2018;10(9):337.

44. Anderson AS, Roberts PC, Frisard MI, Hulver MW, Schmelz EM. Ovarian tumor-initiating cells display a flexible metabolism. *Exp Cell Res*. 2014;328(1):44-57.